The circular movement of synchronous extreme precipitation preceding Kerala floods in 2018 and 2019

Praveenkumar Venkatesan, Gaurav Chopra, Rewanth Ravindran, Shraddha Gupta, Vishnu R. Unni, Norbert Marwan, Jürgen Kurths, R.I. Sujith

Originally published as
Venkatesan, P., Chopra, G., Ravindran, R., Gupta, S., Unni, V.R., Marwan, N., Kurths, J., Sujith, R.I. (2025): The circular movement of synchronous extreme precipitation preceding Kerala floods in 2018 and 2019 . - Chaos, 35, 5, 053115.
https://doi.org/10.1063/5.0246909

Chaos
An Interdisciplinary Journal of Nonlinear Science

RESEARCH ARTICLE | MAY 02 2025

The circular movement of synchronous extreme precipitation preceding Kerala floods in 2018 and 2019

Praveenkumar Venkatesan ; Gaurav Chopra ; Rewanth Ravindran ; Shraddha Gupta ; Vishnu R. Unni ; Norbert Marwan ; Jürgen Kurths ; R. I. Sujith

Chaos 35, 053115 (2025)
https://doi.org/10.1063/5.0246909

The circular movement of synchronous extreme precipitation preceding Kerala floods in 2018 and 2019

Cite as: Chaos 35, 053115 (2025); doi: 10.1063/5.0246909
Submitted: 5 November 2024 · Accepted: 16 April 2025 ·
Published Online: 2 May 2025

Praveenkumar Venkatesan,[1,2] Gaurav Chopra,[1,2] Rewanth Ravindran,[2,3] Shraddha Gupta,[4,5] Vishnu R. Unni,[6] Norbert Marwan,[5,7] Jürgen Kurths,[5,8] and R. I. Sujith[1,2,a)]

AFFILIATIONS

[1]Centre of Excellence for Studying Critical Transitions in Complex Systems, Indian Institute of Technology Madras, Chennai, Tamil Nadu 600036, India
[2]Department of Aerospace Engineering, Indian Institute of Technology Madras, Chennai, Tamil Nadu 600036, India
[3]Department of Civil and Environmental Engineering, Technical University of Darmstadt, Darmstadt 64287, Germany
[4]Department of Geography, Ludwig-Maximilians-Universität München, Munich 80333, Germany
[5]Research Department 4 Complexity Science, Potsdam Institute for Climate Impact Research, Member of the Leibniz Association, Potsdam 14412, Germany
[6]Department of Mechanical and Aerospace Engineering, Indian Institute of Technology Hyderabad, Kandi, Sangareddy, Telangana 502284, India
[7]Institute of Geoscience, University of Potsdam, Potsdam 14476, Germany
[8]Institute of Physics, Humboldt Universität zu, Berlin 10117, Germany

[a)]**Author to whom correspondence should be addressed:** sujith@iitm.ac.in

ABSTRACT

In 2018 and 2019, Kerala, the southernmost state in India, experienced extreme precipitation, leading to appallingly devastating floods that damaged life and property. Kerala is vulnerable to flooding due to its topography, geographical location, and meteorology. Several phenomena have been attributed to these extreme precipitations; however, no single explanation suffices to explain such complex climate phenomena. We view the occurrence of extreme precipitation that leads to floods, such as an emerging phenomenon through the lens of complex system theory. We analyze the patterns of synchrony of extreme fluctuations in precipitation, outgoing longwave radiation, and water vapor transport. We construct time-varying functional climate networks, in which the statistical similarity between the time series of extreme precipitation at different spatial locations is estimated using event synchronization. The network topology reveals that excessive precipitation during the Kerala floods was associated with a coherent pattern of synchronized extreme rainfall. In the coherent phenomena discovered, the extreme rainfall was synchronized across a wide range of length scales spanning 100–1000 km. Furthermore, it traverses a synoptic scale path. After originating in the equatorial Indian Ocean, the coherent pattern moves eastward across the Bay of Bengal. The pattern stops over the Maritime Continent and changes its direction. It moves westward toward the Indian peninsula and accumulates over southwest India. We find that the extreme precipitation was driven by enhanced convective activity, leading to cloudiness and high-vapor transport in the atmosphere. Our findings improve the understanding of intraseasonal variability in the Indian monsoon and extreme precipitation events.

Extreme precipitation (EP) often leads to catastrophic events such as flooding and landslides. Understanding the spatiotemporal dynamics of extreme precipitation is crucial for predicting and developing disaster relief plans. This study focuses on extreme rainfall that happened over Kerala, a state in South India, during the Indian Summer Monsoon in 2018 and 2019. We use complex network analysis to understand the dynamics of extreme precipitation. Complex networks allow us to identify the underlying interactions and self-organizing mechanisms of a system comprised of multiple subsystems, such as our Earth's climate. The network proposed here captures the spatiotemporal dynamics of synchronized extreme precipitation, particularly

their propagation direction and associated time scales. We also find that these extreme events are associated with significant convective activity leading to cloudiness and integrated vapor transport. This understanding may help in anticipating such extreme precipitation well in advance in the future.

I. INTRODUCTION

Extreme weather events deviate significantly from the typical conditions and exhibit unusually intense or severe characteristics. These include heatwaves, droughts, hurricanes, and extreme rainfall. The present study focuses on extreme precipitation associated with large amounts of anomalous precipitation. EPs have become more frequent and intense due to anthropological climate change.[1] Flooding by EP often results in severe infrastructure damage, fatalities, and economic disruption.[2] It affects the availability and quality of freshwater resources, water storage, groundwater recharge, and water availability for various sectors such as agriculture, industry, and domestic use. EPs influence ecosystems and biodiversity by altering habitats, the nutrient cycle, and species distribution.[3] Understanding extreme rainfall patterns, their causes, and their effects facilitates developing effective flood risk management as well as early warning systems and plans of emergency readiness.

Here, we study the EP phenomena in Southwest India during 2018 and 2019, which led to flooding. These floods and the associated landslides affected one-sixth of the inhabitants of Kerala. Hence, these events is referred to as the Kerala floods.[4,5] Over 483 people were killed, 15 went missing, and millions lost their homes.[6] These floods happened during the Indian summer monsoon (ISM). The ISM is associated with the northward shift of the intertropical convergence zone (ITCZ), a planetary scale east–west band of convection, deep clouds, and precipitation.[7] The ITCZ moves toward the Indian subcontinent through Kerala. As a result, the first monsoon onset in the country occurs in Kerala, typically in June. As the ITCZ migrates northward, the rainfall over Kerala subdues. EPs in 2018 and 2019 are intriguing anomalous events because they occurred in August when the ITCZ was located further north.

Several studies have explored the reason behind EP that caused the Kerala floods in 2018. Lyngwa and Nayak[8] attributed the EP and subsequent flooding in Kerala in 2018 to the intense and long-duration category 5 atmospheric river (AR) stretching from the Arabian Sea across South India into the Bay of Bengal. This AR was associated with a moisture flow from the Indian Ocean to Kerala, steered by the depression over the Bay of Bengal. The moisture flow was obstructed by the mountains on the Western Ghats, leading to intense precipitation. This depression resulted from a combined action of a polar westerly jet and monsoon circulation. In contrast, Chaluvadi *et al.*[9] attributed the EP in 2018 to an offshore vortex over the coast of Kerala, which was formed due to the eastward shifting of cross-equatorial flow over the Indian Ocean. This vortex enhanced the moisture transport from the Arabian Sea toward Kerala. Other contributing phenomena were the northward shift and expansion of the western flank of the West Pacific Subtropical High, leading to a blocking high in East Asia. This blocking high resulted in depression over the Bay of Bengal. Kumar *et al.*[10] attributed the 2018 EP to the outcome of an interaction between the offshore trough, low-pressure system, dry air intrusion in the middle troposphere, and other regional features. The mixing of cold–dry air from the Middle East region in the middle troposphere with south-westerly winds in the lower troposphere was sufficient to create an unstable atmosphere during EP. Vijaykumar *et al.*[11] linked EP in Kerala to a mesoscale mini cloudburst event. Kiran[12] related the EP to westward-propagating high-frequency tropical atmospheric waves, which originate near the West Pacific and travel to the east coast of Africa. The cyclonic circulation stimulated convection and supplied continuous moisture along its trajectory. Athira *et al.*[13] attributed the 2018 EP to be unusual moisture transport and ocean–atmosphere coupling over the south equatorial Indian Ocean. Hunt and Menon[4] related EP to the monsoon low-pressure system during 6–9 August 2018 and subsequent monsoon depression during 13–17 August 2018. Suneela *et al.*[14] related the EP to anomalous weather conditions, which include the positive phase of Madden-Julian Oscillation (MJO), a strong low-level jet, a stationary monsoon depression over the Bay of Bengal, a weak offshore trough in the southeast Arabian Sea, the coincidence of the ascending limbs of the Walker and Hadley circulation, the occurrence of the tropical easterly jet, and mid-tropic cyclonic circulation.

In complex systems such as the Earth's climate, extreme events may emerge due to a myriad of nonlinear interactions among its many components across multiple scales.[15,16] Therefore, it is not surprising that the explanation of the physical mechanism underlying the same EP of 2018 has divergent viewpoints. To gain a comprehensive understanding of the climate factors leading to the 2018 Kerala floods, it is essential to consider it from a perspective of the complex system theory. EPs are considered as emergent phenomena arising due to nonlinear interactions and teleconnections in the climate system.[17] Several phenomena, such as moisture availability, atmospheric instability, topography, atmospheric circulation patterns such as the El Niño-Southern Oscillation, the North Atlantic oscillation, and tropical intra-seasonal oscillations, lead to nonlinear interactions that can cause EP. The present work explores the EP that led to the Kerala floods in 2018 and 2019 from a complex systems perspective.

Through a complex networks approach, we embed the climate dynamics into a network (graph) consisting of an ordered set of nodes and links. Nodes are the geographical locations where climate variables are measured, and links represent interactions or connections between nodes. Conventionally, links are established via statistical similarity between dynamics of climate variables occurring at the nodes. Since these networks derive the pattern of interactions via statistical relationships between nodes, they may or may not represent real physical connections and belong to the class of functional complex networks. However, functional networks cannot be used to establish causality because they are based on statistical similarity[18–20] and future climate research should focus on improving methods for describing interactions in climate.

Boers *et al.*[21] reported that the complex networks approach is a robust methodology to unravel teleconnections and interactions in the climate system. Malik *et al.*[22,23] investigated the spatiotemporal characteristics of the ISM using complex networks. Stolbova *et al.*[24] used a complex network approach to determine the topology and evolution of the extreme rainfall network before, during, and after the ISM. Recently, Gupta *et al.*[25] identified the relationship

and synchronization between ISM and East Asian Summer Monsoon using complex network analysis. Boers *et al.*[21,26] used complex networks to investigate the synchronicity of extreme rainfall in the South American monsoon system.

The studies mentioned above suggest that complex network analysis can unravel spatiotemporal patterns of synchronized extreme rainfall.[17,21,24–26] Given that climate is a complex system, analyzing local weather is not sufficient for fully understanding the mechanism behind extreme events. It is critical to understand interactions between constituent components that unravel the emergent large scale phenomena responsible for extreme events. Since interactions are dynamic in nature, we use time-varying complex networks approach.[27] This approach is capable of unraveling such large-scale phenomenon and distinguishing them from local ones. We construct time-varying extreme precipitation networks using event synchronization (ES) measure and study the spatiotemporal patterns before the Kerala floods in the years 2018 and 2019. To further understand the physical processes involved in the extreme precipitation event, we study the dynamics of the outgoing longwave radiation (OLR) and the integrated vapor transport (IVT). OLR and IVT are good measures of deep convective clouds in tropics and moisture flux in the atmosphere, respectively. Since these phenomena are one of the major drivers of extreme rainfall, we explore their roles both individually and along with extreme precipitation in this study.

II. MATERIALS AND METHODS

A. Data

We use ERA5 reanalysis data of total precipitation, OLR, and IVT[28] for each grid point of the geographical area under consideration. The temporal resolution of the data is 3 h. Here, we consider the precipitation, OLR, and IVT data corresponding to the ISM months spanning June, July, and August (JJA) for the years 2018 and 2019 during which the Kerala floods occurred. The spatial extent of the geographical area is 60° E to 110° E and 5° S to 25° N. The spatial resolution of data is 0.5° × 0.5°, and it comprises of 6161 nodes.

B. Construction of functional network using event synchronization (ES)

Due to the dynamic nature of these phenomena in this study, we construct time-varying networks, where the network corresponding to each day is constructed by considering extreme precipitation data for the previous seven days. Since extreme rainfall occurred in August 2018 and 2019, we consider the precipitation data from June to August. A schematic diagram of a time-varying network is shown in Fig. 1. To construct a network, we consider only the wet days (the days with rainfall of more than 1 mm) and then define EP at each node as the days with rainfall greater than the 95th percentile. The percentile method to define events is one of the approaches to characterize extreme events. Moreover, it is robust and less affected by sampling uncertainty.[23,29] To establish the link between two nodes, we use ES, which is a measure of statistical similarity. ES captures the simultaneous occurrence of events across different nodes at the same time or within an appropriate short and flexible interval of time (refer the Appendix for more details about ES). This tool has been successfully implemented in many studies to analyze the local and global patterns of extreme precipitation.[17,21,22,24–26] Each seven-day network is constructed by thresholding the event synchronization matrix Q. We construct an undirected and unweighted network by establishing links if Q_{ij} is above a certain threshold γ. This information is encoded in the adjacency matrix (A), obtained as follows:

$$A_{ij} = \begin{cases} 1 & \text{if } Q_{ij} \geq \gamma, \\ 0 & \text{if } Q_{ij} < \gamma. \end{cases} \quad (1)$$

The present study considers the 95th percentile of the distribution of Q_{ij} as the threshold (γ).[21] The 95th percentile of the Q_{ij}

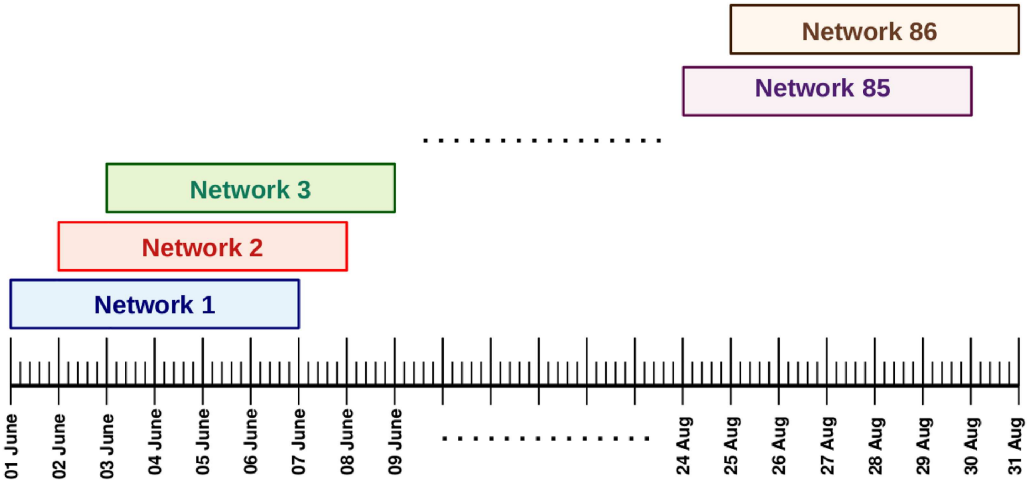

FIG. 1. Schematic diagram of the time-varying network: The network for each day is constructed by considering the time series for the previous 7 days. In total, we constructed 86 networks.

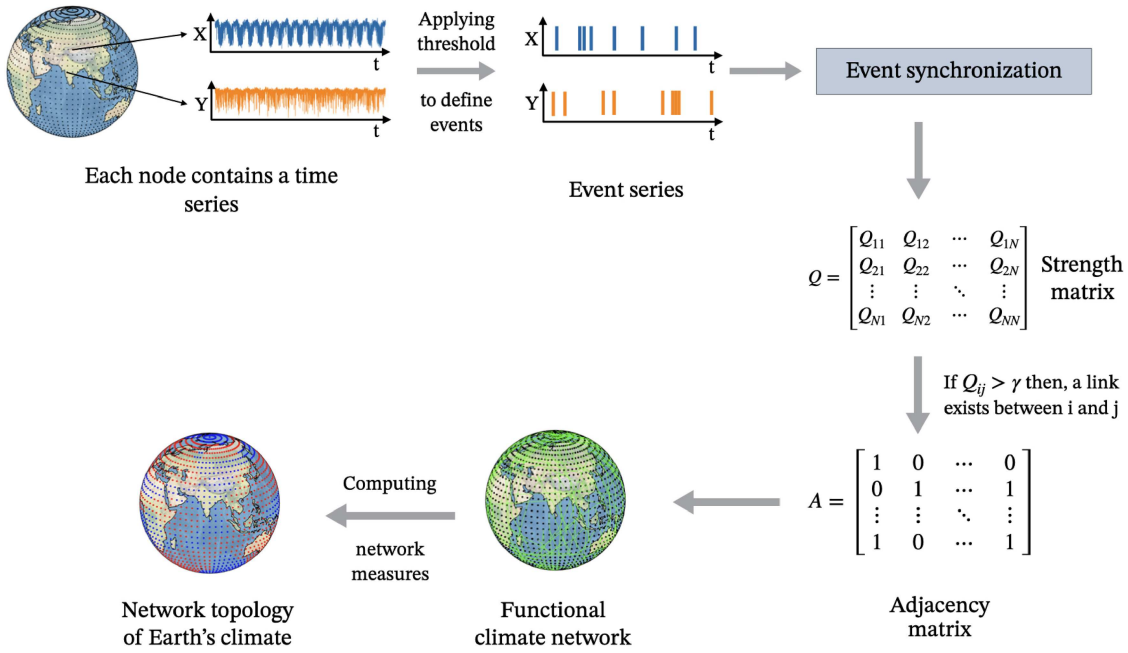

FIG. 2. Workflow adopted for constructing a climate network from extreme precipitation data by employing event synchronization: Each grid point has a precipitation time series. Then, the extreme precipitation for each grid point is identified by thresholding precipitation at the 95th percentile at that grid point. Subsequently, event synchronization is computed between each pair of grid points. This gives an ES strength matrix for each network. The adjacency matrix is constructed by employing a certain threshold on the ES strength matrix.

distribution is different for each network. We calculate the network measures from the adjacency matrix of each seven-day network. The workflow corresponding to the network construction from the precipitation data is shown in Fig. 2.

We have examined the effect of window size by constructing networks using a range of values from 1 to 17 days. Window sizes from 1 to 4 days are not sufficiently large to capture the dynamics of meso-scale activity. The window size range of 5–10 days captures the relevant patterns as well as their propagation. However, larger window sizes, 11–17 days, the meso-scale activity and its propagation are smeared in the patterns, making them inappropriate for tracking. Therefore, we consider the window size of seven days in this study.

C. Network measures

Since we are interested in the spatial regions that exhibit similar behavior, we compute the degree. The degree is a node-based network measure that quantifies how many other nodes exhibit similar behavior. The degree (k_i) of a node i is defined as the number of connections it has to all other nodes,

$$k_i = \sum_{j=1}^{n} A_{ij}, \tag{2}$$

where n is the total number of nodes.

D. Statistical significance test

We test the statistical significance of the ES between two connected nodes ($S_{ij} \geq 95\%$) by performing a random permutation surrogate test.[30] We construct 100 surrogates for one node by randomly shuffling the original precipitation event series. Next, we calculate the ES between the surrogates and the original time series of the other node. We consider only those pairs of nodes to be connected for which $S_{ij} \geq 95\%$.

III. RESULTS

The southwest coast of India experienced anomalous rainfall in August 2018 and 2019 that led to the catastrophic Kerala floods. In both years, excessive rainfall occurred in two phases. In 2018, the first spell occurred from 8 to 10 August, and the second one from 14 to 17 August. Meanwhile, in 2019, the first spell was observed from 5 to 10 August and the second from 18 to 26 August. The intensity of the rainfall was observed to be unequal during the two spells. In 2018, the second spell experienced higher rainfall than the first. On the other hand, in 2019, the first spell was stronger. Figures 3(a)–3(d) show the spatial distribution of monthly averaged precipitation and anomalous precipitation of August for both years, respectively.[9,12] The anomalous rainfall was much higher in 2019 than in 2018 over Kerala.

(i) 2018: The spatial distributions of the degree of extreme precipitation network for certain dates in 2018 are shown in

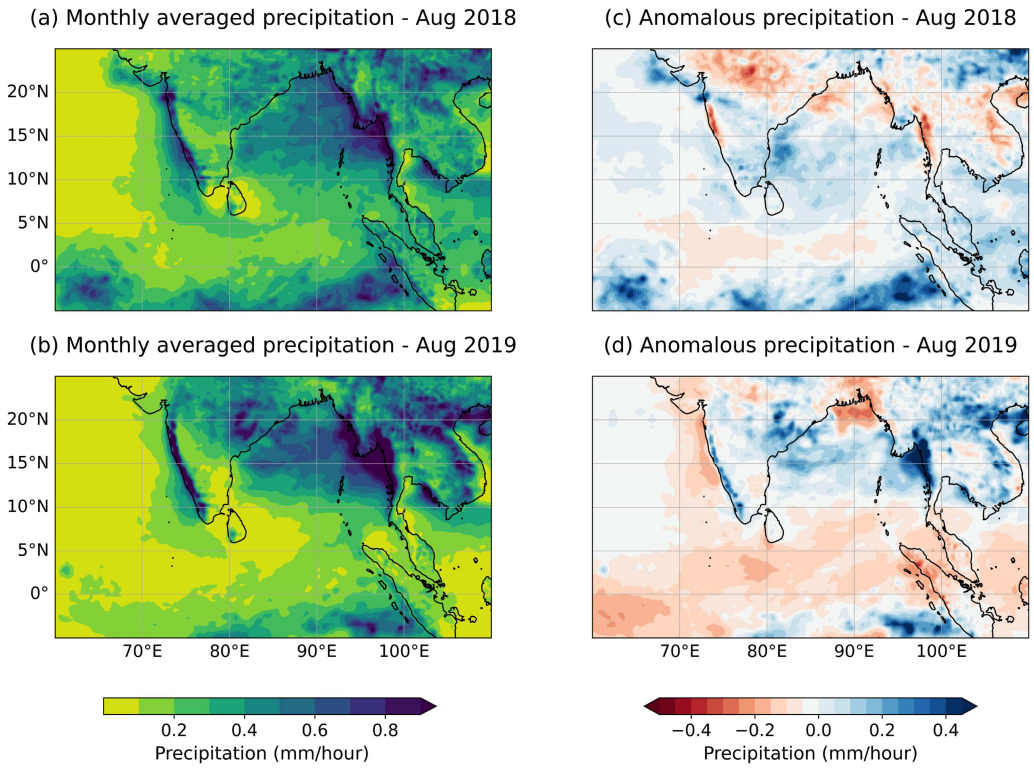

FIG. 3. The spatial distribution of monthly averaged precipitation and monthly averaged anomalous precipitation: (a) and (b) show the monthly averaged precipitation of August 2018 and August 2019, respectively. (c) and (d) show the monthly anomalous precipitation of August 2018 and August 2019, respectively. The west coast of Kerala received more rainfall than usual in August 2018 and 2019.

Figs. 4(a)–4(f) (Multimedia available online). The blue box highlights the critical region of synchronized extreme precipitation (RSEP) that was responsible for the anomalous rainfall over the southwest coast of India and subsequent Kerala floods. The arrow marks the circulatory trajectory followed by the RSEP. The arrows are drawn by visual inspection. We show the point-to-point ES strength between the EP and the OLR and between the EP and the IVT for 2018 in Figs. 4(g)–4(l) and 4(m)–4(r), respectively. The OLR is the long wavelength thermal radiation emitted to space at the top of the atmosphere. A low value of OLR in the tropics corresponds to the presence of deep convective clouds, while a high value of OLR corresponds to their absence.[7,31] Here, we consider the value of OLR, which is less than 210 Wm^{-2}, as an event, and then estimate ES between EP and OLR with the same node using

$$ES_{i_{EP}j_{OLR}} = \frac{C(i_{EP}|j_{OLR}) + C(i_{OLR}|j_{EP})}{\sqrt{(s_{EP}-2)(s_{OLR}-2)}}. \quad (3)$$

IVT gives information about the flow rate of water vapor through a column of air extending from the surface of the Earth to the top of the atmosphere. We apply the 95th percentile threshold to IVT data to create an event series; then, we estimate ES between EP and IVT as

$$ES_{i_{EP}j_{IVT}} = \frac{C(i_{EP}|j_{IVT}) + C(i_{IVT}|j_{EP})}{\sqrt{(s_{EP}-2)(s_{IVT}-2)}}. \quad (4)$$

We find that on 26th July 2018 [in Fig. 4(a)], the RSEP originates over the central part of the Indian Ocean. In Figs. 4(g) and 4(m), we observe that the RSEP is associated with a high synchronization between EP-OLR and EP-IVT. This indicates that the RSEP is associated with local convective activity and atmospheric vapor transport. Then, the RSEP moves northeast and accumulates over the South China Sea from 31st July to 10th August [in Fig. 4(c)]. Meanwhile, initially, the degree starts to decrease, and in the subsequent days, the degree increases. On the contrary, the ES between EP-OLR and EP-IVT decreases. The decrease in ES between the EP-IVT is significant compared to that of EP-OLR, indicating that the contribution of vapor transport activity becomes lower than the convective activity. Further, beyond the day 10th August, the ES patterns of EP-IVT become sparser than those of EP-OLR, indicating that the convective activity occurs at a relatively larger spatial scale and is much more organized than the vapor transport activity. Next, RSEP moves west and reaches the South Indian Peninsula by 17th August. Extreme precipitation during the phase of the RSEP movement from 17th to 20th August led to Kerala floods in 2018. This southward movement of RSEP is because of North–South wind in

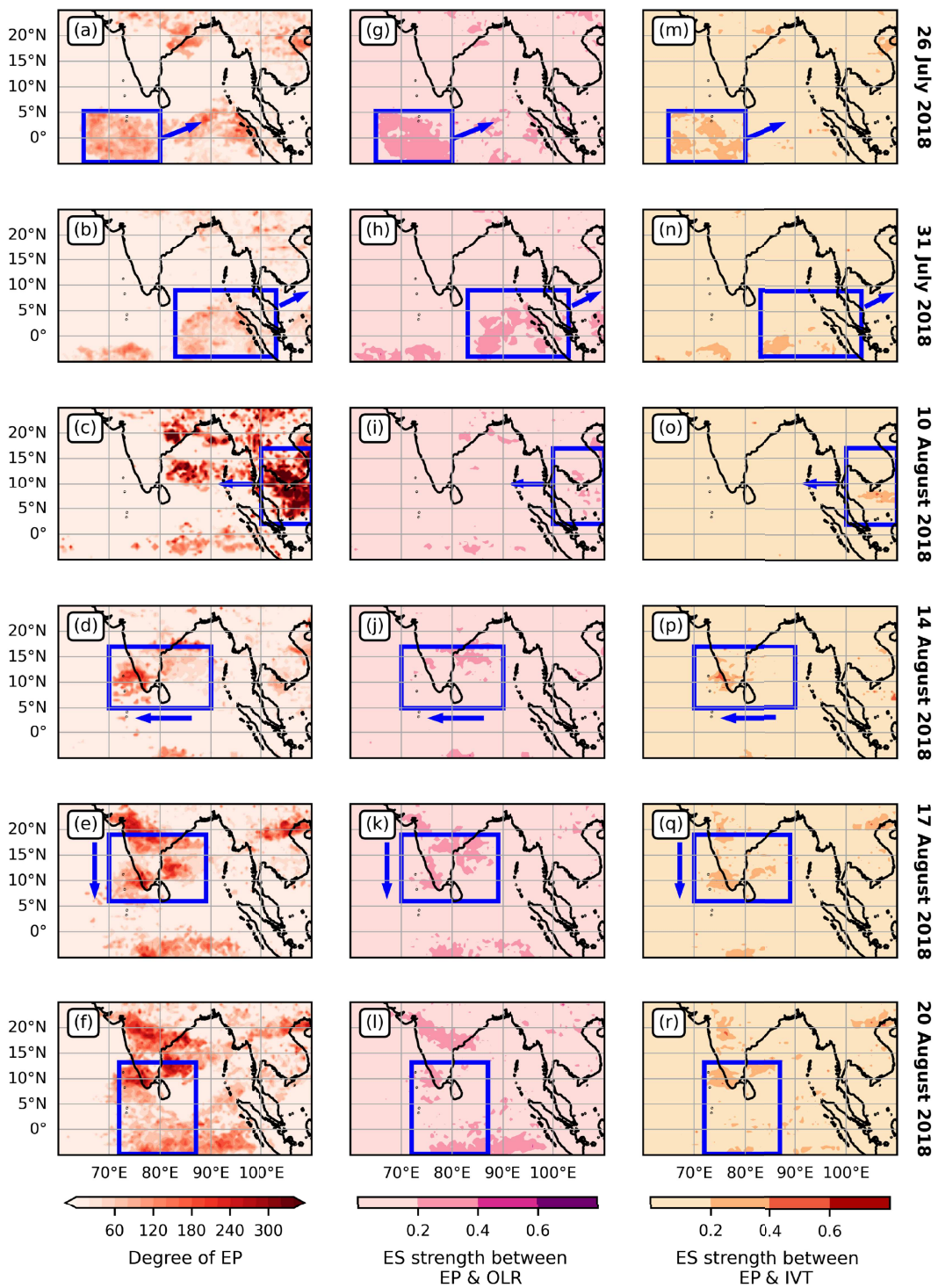

FIG. 4. Spatial distribution of the degree of (a)–(f) synchronized extreme precipitation network (left panel), (g)–(l) point-to-point ES strength between EP and OLR (middle panel), and (m)–(r) between EP and IVT (right panel) for the year 2018. The blue boxes highlight the critical region of synchronized extreme rainfall. Animation for figures (a)–(f) is available online. Multimedia available online.

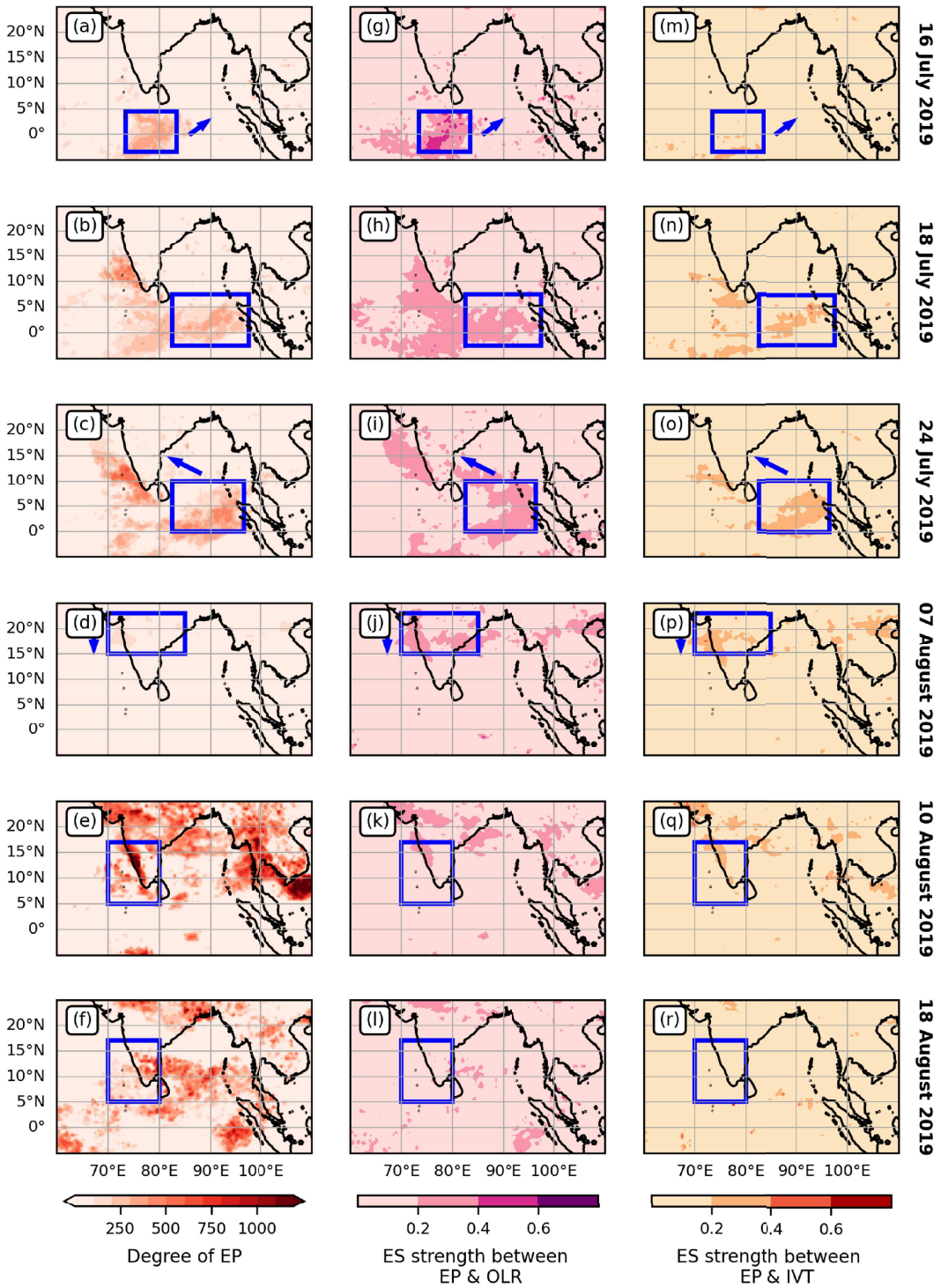

FIG. 5. Spatial distribution of the degree of (a)–(f) synchronized extreme precipitation network (left panel), (g)–(l) point-to-point ES strength between EP and OLR (middle panel), and (m)–(r) between EP and IVT (right panel) for the year 2019. The blue boxes highlight the critical region of synchronized extreme rainfall. Animation for figures (a)–(f) is available online. Multimedia available online.

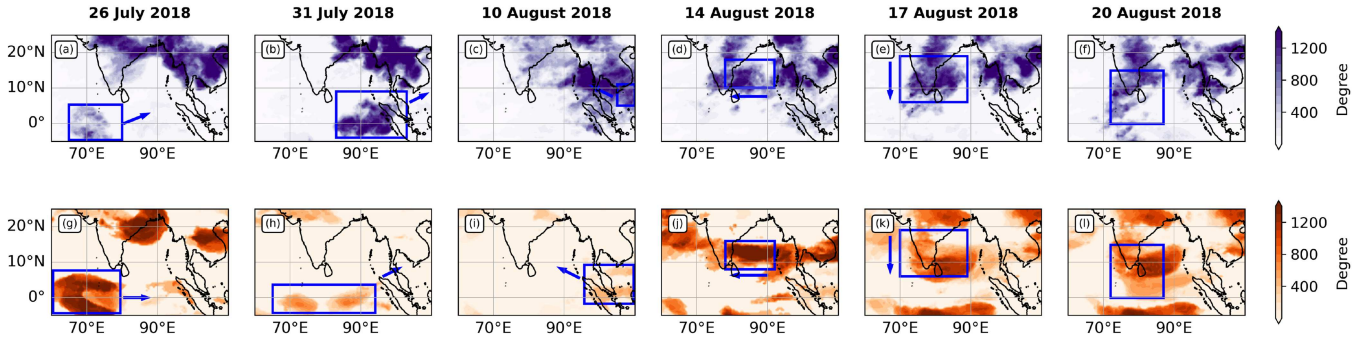

FIG. 6. Spatial distribution of degree for time-varying networks of (a)–(f) OLR (top panel) and (g)–(i) IVT (lower panel) for the year 2018.

this region caused by cyclonic vorticity over the Bay of Bengal. In Figs. 4(l) and 4(r), the synchronization between EP-OLR and EP-IVT along the southwest coast of India is high during this phase. Thus, both convective and vapor transport activities were important in causing EP. The RSEP took around 30 days to complete the circulatory pattern.

(ii) 2019: In 2019, the RSEP originates over the central part of the Indian Ocean on 16th July [in Fig. 5(a)] [Multimedia available online for the figures from (a) to (f)], showing a strong association with convection activity rather than vapor transport, since we observe a similar pattern in EP-OLR [Fig. 5(g)]. In the subsequent days, its strength increases, along with ES strength of both EP-OLR and EP-IVT, and the RSEP spreads over the Indian Ocean by 18th July [Fig. 5(b)]. Further, it moves in the northeastern direction. It reaches the west coast of Indonesia by 24th July [Fig. 5(c)], where the EP is highly synchronized with convective activity and vapor transport. Furthermore, RSEP moves toward the Indian Peninsula and reaches there by 7th August [Fig. 5(d)] while its strength decreases even though the ES strengths between EP-OLR and EP-IVT are high. The movement of RSEP from August 7th to August 18th [Figs. 5(d)–5(f)] led to extreme rainfall in Kerala in two phases. During the first phase of the extreme rainfall [Fig. 5(e)], it is associated with both convective activity and vapor transport, which can be seen in Figs. 5(k) and 5(q). In contrast, during the second phase on August 18th [Figs. 5(f), 5(l), and 5(r)], ES strength between EP-OLR, and EP-IVT is low in the region of RSEP indicating some other phenomena at play.

Next, in order to understand the physical mechanism behind the EP spatiotemporal pattern, we investigate the convective activity and water vapor transport over the region for the considered time period. In Figs. 6 and 7, we show the degree of the OLR and IVT networks for both years, respectively. Both the convective activity and vapor transport exhibit a similar kind of circulatory pattern observed in the EP network. For 2018, in the initial phase of the circulatory pattern of convective activity, we find two dominant convective patterns over the region of interest [Fig. 6(b)]; the northern one corresponds to the ITCZ, and the southern one is anomalous, which performs the circulatory movement and causes EP over Kerala. The northern convective band moves southeast, while the southern one moves northeast and both converge toward the Maritime Continent. On 10th August, the northern and southern bands merge over the Maritime Continent. Thereafter, part of the merged band moves west toward the Indian peninsula. In contrast, in 2019, the northern band is relatively weaker compared to that for 2018. Meanwhile, the southern one performs a similar movement as in 2018.

In Fig. 8, we show the schematic pathway of the synchronized extreme rainfall. For both years, the movement of RSEP originates

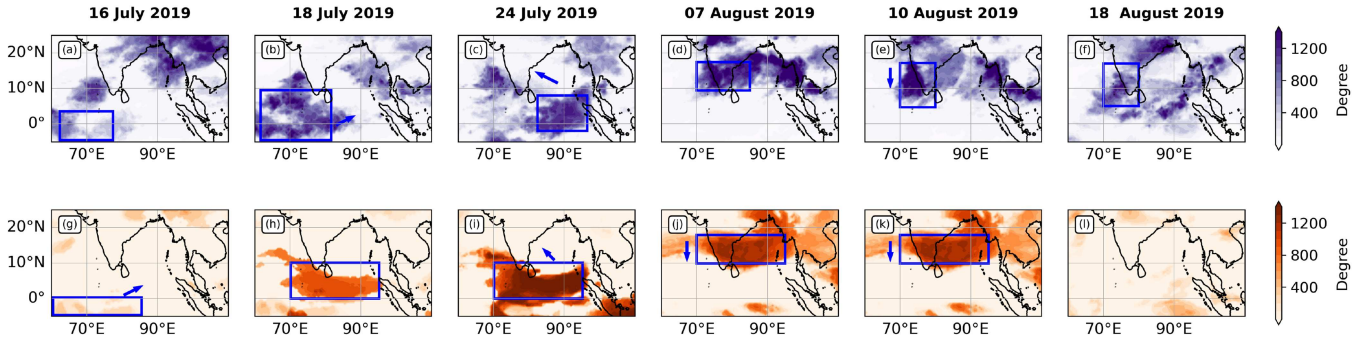

FIG. 7. Spatial distribution of degree for time-varying networks of (a)–(f) OLR (top panel) and (g)–(i) IVT (lower panel) for the year 2019.

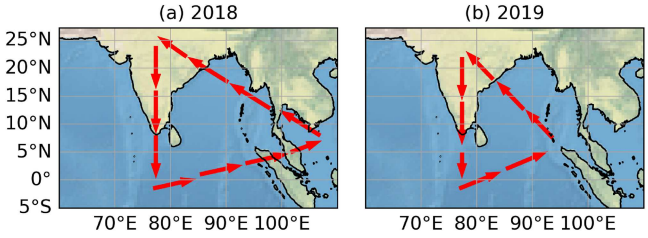

FIG. 8. Schematic of the path (red arrows) followed by RSEP in (a) 2018 and (b) 2019.

and ends in the Central Indian Ocean. In 2018, the propagation of extreme rainfall covered a larger region than in 2019. The circulatory patterns of regions having a high degree are associated with low OLR and high IVT. We do not observe circulatory patterns in other years except 2018 and 2019. For reference, we have included an animation of the spatial distribution of the degree of the time-varying network of extreme precipitation JJA for the year 2015 in the supplementary material.

IV. CONCLUSION

We investigate the anomalous EP along the southwest coast of India, especially over Kerala, that led to catastrophic floods in 2018 and 2019 from the perspective of complex systems theory. This approach enables unraveling hidden interactions and self-organized patterns in the climate that lead to rare extreme events such as EP. We construct time-varying functional networks whose nodes are the geographical locations in the spatial domain spanning 60° E to 110° E and 5° S to 30° N. Links representing interactions are established by calculating the statistical similarity between event time series of climate variables of nodes. We use event synchronization as the statistical similarity measure, which estimates the nonlinear synchronization between two event time series. We construct three types of networks based on different climatic parameters precipitation, OLR and IVT. At a given node, instants of precipitation and IVT greater than the 95th percentile are regarded as an event. We then track the convective activity using OLR, since it is a good proxy for deep convective clouds within the tropics. Deep convective clouds have OLR $< 210\,\mathrm{W/m^2}$, and we consider this value as the threshold for constructing event time series.

Earlier studies have attributed these extreme precipitations to the landfall of category 5 atmospheric rivers[8] and changes in large-scale circulations in the Indo-Pacific ocean zone.[9] In contrast to these studies, we explore the extreme rainfall events from a complex systems perspective using the complex networks approach. We discover that these events are associated with a larger self-organized system of synchronized extreme rainfall. This system originates in the Indian Ocean propagates through the Bay of Bengal and the South China Sea and eventually ends up over southern India, leading to Kerala floods in 2018 and 2019. Furthermore, we find that the corresponding anomalous extreme rainfall was caused by enhanced convective activity and integrated vapor transport. Further, we have investigated the role of boreal summer intraseasonal oscillations[32] (BSISOs) by exploring the spatiotemporal patterns of the reconstructed *OLR* anomaly. This way we have found that the deep cloudiness associated with the BSISO activity was weak over Kerala during extreme rainfall events. Furthermore, our analysis has a strong potential to develop precursors and early warning models for such events. This may be achieved in practice by using the pattern recognition technique involving machine learning, by looking for similar circulatory patterns in the region of study. Identifying a precursor would enable us to do preparatory actions.

SUPPLEMENTARY MATERIAL

In the supplementary material, we have included multimedia (video) of the circulatory pattern of extreme precipitation for the years 2015, 2018, and 2019.

ACKNOWLEDGMENTS

P.V., G.C., and R.I.S. are grateful for the funding and support provided by the Office of Naval Research Global (O.N.R. Global) under Grant No. SP21221684AEONRG002696 (Contract monitor: Dr. Derrick Marcus Tepaske). V.R.U. is grateful for the Startup Research Grant—IIT Hyderabad. The authors are grateful to Mrs. Shruti Tandon, Ph.D. student at IIT Madras, Dr. Praveen Kasthuri, a former Ph.D. student at IIT Madras, and Dr. Tobias Braun, a post-doctoral researcher at Potsdam Institute for Climate Impact Research, Germany, for fruitful suggestions and comments.

AUTHOR DECLARATIONS

Conflict of Interest

The authors have no conflicts to disclose.

Author Contributions

Praveenkumar Venkatesan: Data curation (lead); Formal analysis (lead); Methodology (equal); Visualization (lead); Writing – original draft (lead). **Gaurav Chopra:** Conceptualization (equal); Data curation (equal); Formal analysis (equal); Methodology (equal); Visualization (equal); Writing – original draft (equal). **Rewanth Ravindran:** Data curation (equal). **Shraddha Gupta:** Formal analysis (equal); Writing – review & editing (equal). **Vishnu R. Unni:** Formal analysis (equal); Methodology (equal); Writing – review & editing (equal). **Norbert Marwan:** Writing – review & editing (equal). **Jürgen Kurths:** Writing – review & editing (equal). **R. I. Sujith:** Conceptualization (equal); Formal analysis (equal); Methodology (equal); Project administration (equal); Supervision (equal); Writing – original draft (equal); Writing – review & editing (equal).

DATA AVAILABILITY

The ERA5 Reanalysis data[28] that we used in this study are openly available in Copernicus at https://cds.climate.copernicus.eu/, Ref. 28.

APPENDIX: EVENT SYNCHRONIZATION (ES)

ES is a nonlinear measure to estimate the relationship between event series at different geographic locations.[33] Consider two locations, i and j, and estimate the extreme rainfall events (t_l^i and t_m^j) from their respective precipitation time series by applying the α percentile threshold. l and m vary from $1, \ldots, s_i$ and $1, \ldots, s_j$, respectively. Here, s_i and s_j are the total number of extreme precipitation events in the time series of grid points i and j, respectively. Next, we estimate the dynamic delay (τ) between two-time series as follows:

$$\tau_{lm}^{ij} = \frac{\min\left(t_l^i - t_{l-1}^i, t_{l+1}^i - t_l^i, t_m^j - t_{m-1}^j, t_{m+1}^j - t_m^j\right)}{2}. \tag{A1}$$

Here, τ_{lm}^{ij} is a dynamic delay representing the shortest time interval between successive and preceding events. In this study, we defined the maximum dynamic delay $[\tau_{lm}]_{\max}$ as one day. If the dynamic delay τ_{lm} exceeds $[\tau_{lm}]_{\max}$, then we set it to $[\tau_{lm}]_{\max}$; otherwise, the calculated dynamics delay (τ_{lm}) will be used for further analysis,

$$\tau_{lm} = \begin{cases} 1 & \text{if } \tau_{lm} > 1 \text{ day}, \\ \tau_{lm} & \text{if } \tau_{ij} < 1 \text{ day}. \end{cases} \tag{A2}$$

If the events between two grid points i and j fall within τ_{lm}^{ij}, it is considered to be synchronized. In other words, if two geographical locations receive extreme rainfall within a day, this is considered to be synchronized extreme rainfall. If there are no rainfall events throughout the day, then we consider that there is no synchronized extreme rainfall. We construct a strength matrix with all nodes for each of the seven days by repeating the above-mentioned process for all (6161) grid points. The number of synchronized events between i and j, ($c(i|j)$) and vice versa ($c(j|i)$) are estimated as follows:

$$c(i|j) = \sum_{l=1}^{s_i} \sum_{m=1}^{s_j} J_{ij}^{lm}. \tag{A3}$$

Here, J_{ij}^{lm} are the weights defined as

$$J_{ij}^{lm} = \begin{cases} 1 & \text{if } 0 < t_l^i - t_m^j \le \tau, \\ \frac{1}{2} & \text{if } t_l^i - t_m^j = 0, \\ 0 & \text{else.} \end{cases} \tag{A4}$$

In this way, we avoid counting the paired events twice if they occur at the exact same time. Next, we estimate the strength of event synchronization using

$$Q_{ij} = \frac{c(i|j) + c(j|i)}{\sqrt{(s_i - 2)(s_j - 2)}}. \tag{A5}$$

According to Eq. (A5), Q is a symmetric matrix, and it varies from 0 to 1. $Q_{ij} = 0$ implies no synchronization between points i and j, while $Q_{ij} = 1$ implies complete synchronization. We have tested the effect of $[\tau_{lm}]_{\max}$ on the results. There is no significant qualitative change in the results when the $[\tau_{lm}]_{\max}$ varied from 0.5 to 7 days.

REFERENCES

[1] S. Westra, H. Fowler, J. Evans, L. Alexander, P. Berg, F. Johnson, E. Kendon, G. Lenderink, and N. Roberts, "Future changes to the intensity and frequency of short-duration extreme rainfall: Future intensity of sub-daily rainfall," Rev. Geophys. **52**, 522–555, https://doi.org/10.1002/2014RG000464 (2014).
[2] M. H. Daba and S. You, "Assessment of climate change impacts on river flow regimes in the upstream of Awash Basin, Ethiopia: Based on IPCC fifth assessment report (AR5) climate change scenarios," Hydrology **7**, 98 (2020).
[3] L. Li, Z. Zheng, J. A. Biederman, C. Xu, Z. Xu, R. Che, Y. Wang, X. Cui, and Y. Hao, "Ecological responses to heavy rainfall depend on seasonal timing and multi-year recurrence," New Phytol. **223**, 647–660 (2019).
[4] K. M. Hunt and A. Menon, "The 2018 Kerala floods: A climate change perspective," Clim. Dyn. **54**, 2433–2446 (2020).
[5] S. Nambudri, *Rare Phenomenon in Kerala Caused 2019 Flood* (The Times of India, 2019).
[6] V. Mishra, J. Nanditha, S. Dangar, D. S. Chuphal, and U. Vegad, "Drivers, changes, and impacts of hydrological extremes in India: A review," Wiley Interdiscip. Rev.: Water **11**, e1742 (2024).
[7] S. Gadgil and M. Rajeevan, "The Indian monsoon," Resonance **13**, 1117–1132 (2008).
[8] R. V. Lyngwa and M. A. Nayak, "Atmospheric river linked to extreme rainfall events over Kerala in August 2018," Atmos. Res. **253**, 105488 (2021).
[9] R. Chaluvadi, H. Varikoden, M. Mujumdar, S. Ingle, and J. Kuttippurath, "Changes in large-scale circulation over the Indo-Pacific region and its association with 2018 Kerala extreme rainfall event," Atmos. Res. **263**, 105809 (2021).
[10] V. Kumar, P. K. Pradhan, T. Sinha, S. V. B. Rao, and H.-P. Chang, "Interaction of a low-pressure system, an offshore trough, and mid-tropospheric dry air intrusion: The Kerala flood of August 2018," Atmosphere **11**, 740 (2020).
[11] P. Vijaykumar, S. Abhilash, A. Sreenath, U. Athira, K. Mohanakumar, B. Mapes, B. Chakrapani, A. Sahai, T. Niyas, and O. Sreejith, "Kerala floods in consecutive years—Its association with mesoscale cloudburst and structural changes in monsoon clouds over the west coast of India," Weather Clim. Extremes **33**, 100339 (2021).
[12] S. R. Kiran, "Convectively-coupled high-frequency atmospheric waves triggered Kerala floods in 2018 and 2019," SSRN Electron. J. **2022**, 1–6.
[13] U. Athira, S. Abhilash, and R. Ruchith, "Role of unusual moisture transport across equatorial Indian Ocean on the extreme rainfall event during Kerala flood 2018," Dyn. Atmos. Oceans **95**, 101225 (2021).
[14] S. Suneela, B. Mathew, and S. Sureshkumar, "The anomalous weather parameters that lead to the extreme rainfall of Kerala in August 2018," Meteorol. Atmos. Phys. **135**, 37 (2023).
[15] C. L. E. Franzke and T. J. O'Kane, *Nonlinear and Stochastic Climate Dynamics* (Cambridge University Press, 2017).
[16] A. F. Siegenfeld, and Y. Bar-Yam, "An introduction to complex systems science and its applications," Complexity **2020**, 1–16 (2020).
[17] N. Boers, B. Goswami, A. Rheinwalt, B. Bookhagen, B. Hoskins, and J. Kurths, "Complex networks reveal global pattern of extreme-rainfall teleconnections," Nature **566**, 373–377 (2019).
[18] H. Dijkstra, E. Hernández-García, C. Masoller, and M. Barreiro, *Networks in Climate* (Cambridge University Press, 2019).
[19] J. F. Donges, Y. Zou, N. Marwan, and J. Kurths, "Complex networks in climate dynamics: Comparing linear and nonlinear network construction methods," Eur. Phys. J. Spec. Top. **174**, 157–179 (2009).
[20] J. Fan, J. Meng, J. Ludescher, X. Chen, Y. Ashkenazy, J. Kurths, S. Havlin, and H. J. Schellnhuber, "Statistical physics approaches to the complex earth system," Phys. Rep. **896**, 1–84 (2021).
[21] N. Boers, B. Bookhagen, N. Marwan, J. Kurths, and J. Marengo, "Complex networks identify spatial patterns of extreme rainfall events of the South American monsoon system," Geophys. Res. Lett. **40**, 4386–4392, https://doi.org/10.1002/grl.50681 (2013).
[22] N. Malik, B. Bookhagen, N. Marwan, and J. Kurths, "Analysis of spatial and temporal extreme monsoonal rainfall over South Asia using complex networks," Clim. Dyn. **39**, 971–987 (2012).
[23] N. Malik, N. Marwan, and J. Kurths, "Spatial structures and directionalities in monsoonal precipitation over South Asia," Nonlinear Processes Geophys. **17**, 371–381 (2010).

[24]V. Stolbova, P. Martin, B. Bookhagen, N. Marwan, and J. Kurths, "Topology and seasonal evolution of the network of extreme precipitation over the Indian subcontinent and Sri Lanka," Nonlinear Processes Geophys. **21**, 901–917 (2014).
[25]S. Gupta, Z. Su, N. Boers, J. Kurths, N. Marwan, and F. Pappenberger, "Interconnection between the Indian and the East Asian summer monsoon: Spatial synchronization patterns of extreme rainfall events, Int. J. Climatol. **43**, 1034–1049 (2023).
[26]N. Boers, A. Rheinwalt, B. Bookhagen, H. M. Barbosa, N. Marwan, J. Marengo, and J. Kurths, "The South American rainfall dipole: A complex network analysis of extreme events," Geophys. Res. Lett. **41**, 7397–7405, https://doi.org/10.1002/2014GL061829 (2014).
[27]S. Gupta, N. Boers, F. Pappenberger, and J. Kurths, "Complex network approach for detecting tropical cyclones," Clim. Dyn. **57**, 3355–3364 (2021).
[28]H. Hersbach *et al.*, *ERA5 Hourly Data on Pressure Levels From 1940 to Present* [Copernicus Climate Change Service (C3S), Climate Data Store (CDS), 2018].
[29]D. Burić and M. Doderović, "Trend of percentile climate indices in Montenegro in the period 1961–2020," Sustainability **14**, 12519 (2022).
[30]G. Lancaster, D. Iatsenko, A. Pidde, V. Ticcinelli, and A. Stefanovska, "Surrogate data for hypothesis testing of physical systems," Phys. Rep. **748**, 1–60 (2018).
[31]S. Gadgil, "The Indian monsoon and its variability," Annu. Rev. Earth Planet. Sci. **31**, 429–467 (2003).
[32]K. Kikuchi, "The boreal summer intraseasonal oscillation (BSISO): A review," J. Meteorol. Soc. Jpn. Ser. II **99**, 933–972 (2021).
[33]R. Q. Quiroga, T. Kreuz, and P. Grassberger, "Event synchronization: A simple and fast method to measure synchronicity and time delay patterns," Phys. Rev. E **66**, 041904 (2002).